Droplet model of plasma resonances in medium-size metal clusters

F. Iachello* and E. Lipparini
Dipartimento di Fisica, Università di Trento, 38050 Povo, Italy

A. Ventura
Comitato Nazionale per l'Energia Nucleare e le Energie Alternative, I-40138 Bologna, Italy
(Received 8 February 1991)

We study photon absorption and scattering by medium-size $N=8-20$ sodium clusters, making use of the interacting boson model to describe the coupling of plasma resonances to surface oscillations and deformations of a dropletlike structure. With reasonable assumptions on the nature of the plasma resonances and their couplings, we obtain an excellent description of the experimental photoabsorption data.

I. INTRODUCTION

Recently, systematic studies of photoabsorption spectra of metallic clusters have been performed. A very extensive study of sodium clusters within the size range $N=3-40$ atoms has been presented.[1] With the availability of these studies, it begins to be possible to understand the structural properties of metallic clusters. This problem is of particular importance in view of the fact that clusters bridge the gap between small molecules and infinite systems (crystals). With this article, we begin a systematic investigation of photoabsorption spectra of metallic clusters with the aim of covering the entire range, from the free atom, $N=1$, to the crystal, $N\rightarrow\infty$. Here, we concentrate our attention on medium-size sodium clusters, $N=8-20$, whose spectra have been interpreted as collective excitations of the valence electrons similar to the collective excitations of valence nucleons in atomic nuclei. The multipeak structure observed in the spectrum has been interpreted as evidence for a nonsphericity of the electron cloud.[2] However, a simple ellipsoidal shell model[3] is not able to reproduce the observed spectra for clusters containing $N\geq 13$ atoms.[1] This may be either due to further fragmentation caused by the long-range nature of the Coulomb interaction, which, differently from the nuclear case, can strongly couple the surface-plasma resonance to individual electronic levels,[4] or to the fact that for these medium-size clusters the molecular structure still plays a role, causing a fragmentation of the plasmon modes which follows the discrete symmetry of the clusters. The coupling to other electronic levels has been studied in the random-phase approximation (RPA) in spherical clusters,[4,5] predicting in Na_{20} the occurrence of two closely spaced collective excitations sharing about 70% of the total oscillator strength. Recent *ab initio* calculations[6] of small clusters ($N=4$) also show a multipeak fragmentation that cannot be accounted for by a *single* surface plasmon.

With the aim of studying in detail metallic clusters of any size and structure, we introduce in the following section an algebraic model of plasma resonances similar to those used previously to study nuclear[7] and molecular[8] structure. In this model, the photoabsorption spectrum is obtained by diagonalizing the Hamiltonian

$$\hat{H}=\hat{H}_B+\hat{H}_P+\hat{V}_{B,P}\ . \tag{1}$$

where $\hat{H}_B$ describes the structure of the cluster, $\hat{H}_P$ the plasma resonance, and $\hat{V}_{B,P}$ the interaction between the plasma resonance and the cluster structure. The first term in (1) has been written as $\hat{H}_B$ since the quantal treatment of the oscillations and rotations of the cluster is done in terms of boson operators. Hence, the name interacting boson models (IBM's) is given to this type of model. Here we consider the simple case in which the cluster is described not by a molecular structure, but by a dropletlike structure with an ellipsoidal shape similar to that of atomic nuclei, and show that the assumption of the existence of *two* dipole collective states is able to explain very accurately the observed peak structure in the wavelength range 450–630 nm without the need to invoke nonaxially symmetric shapes. We note that we have also attempted a description in terms of only *one* dipole collective state and triaxial droplet shapes, but were unable to achieve a similar accurate description. The situation seems to be similar to the nuclear case, where triaxiality rarely occurs, if at all.

Having fixed the parameters of the model on photoabsorption data, we also compute (and thus predict) the cross sections for coherent elastic scattering of unpolarized radiation.

II. MODEL

In this paper we take a particular choice of $\hat{H}_B$ in (1), namely that corresponding to the quantization of vibrations and rotations of a classical shape (interacting boson model).[7] If the shape is ellipsoidal with radius

$$R=R_0\left[1+\sum_{\mu}\alpha_{2\mu}Y_{2\mu}(\theta,\varphi)\right]\ , \tag{2}$$

it can be quantized by means of quadrupole bosons (d bosons), having angular momentum and parity $L^{\pi}=2^{+}$. In addition to the five independent quadrupole degrees of freedom, characterized by the creation operators $d^{\dagger}_{\mu}(\mu=-2,-1,0,+1,+2)$, a monopole degree of freedom (s boson) with $L^{\pi}=0^{+}$ is also introduced to take into account the finite size of the system and its volume conservation. With s and d bosons, this leads to conser-

vation of the total number of bosons, N_B. In addition, the introduction of both s and d bosons allows one to treat easily both spherical and deformed clusters, and it is thus crucial for the situation analyzed in this paper. Conversely, the introduction of only d bosons, as in Ref. 9, can easily address the problem of spherical clusters.

The dipole collective states, higher in energy than the quadrupole surface modes, are quantized in terms of p bosons, with angular momentum and parity $L^{\pi}=1^{-}$. The coupling of these to the quadrupole modes—that is, d and s bosons—splits the dipole excitation. The splitting of the plasmon mode turns out, then, to be identical to the splitting of the so-called giant dipole resonance in nuclei. The IBM treatment of this problem by Maino *et al.*[10] is extensively reviewed in Ref. 11. However, a modification of this treatment is necessary, since, as mentioned above, RPA and *ab initio* molecular calculations point to the occurrence of plasmon modes of several types. Here we consider the case of (plasmon) p bosons of two types and droplet ellipsoidal shapes with axial symmetry. In this case, each type is split into two main components due to the coupling to the deformation of the droplet. The situation is somewhat similar to that encountered in the giant resonances of light atomic nuclei where the two plasmon modes are the two different isospin components of the giant resonance.[12] In other words, the two plasmon types are built from configurations with different symmetry properties under particle permutations. The choice of two plasmon types appears to describe the available data in the wavelength range 450–630 nm quite accurately. Generalization to the case of a number of p bosons greater than two and to their splitting in the presence of triaxial shapes is straightforward within the framework of the IBM.

In this work, we use the following boson Hamiltonian[7]

$$\hat{H}_B = E_0 + \varepsilon_d \hat{n}_d + k\hat{\mathbf{Q}}\cdot\hat{\mathbf{Q}} , \tag{3}$$

where E_0 is a c number, such that the ground state has zero energy, and the operators $\hat{n}_d$ and $\hat{\mathbf{Q}}$ are defined in terms of creation and annihilation operators of d bosons, $d^{\dagger}_{\mu}(\mu=-2,\ldots,+2)$ and $\tilde{d}_{\mu}\equiv(-1)^{\mu}d_{-\mu}$, respectively, as well as s bosons, $s^{\dagger}$ and $\tilde{s}\equiv s$. More precisely,

$$\hat{n}_d = (d^{\dagger}\cdot\tilde{d}) \tag{4}$$

is the number operator of d bosons, and

$$\hat{Q}_{\mu} = (d^{\dagger}\times\tilde{s} + s^{\dagger}\times\tilde{d})^{(2)}_{\mu} + \chi(d^{\dagger}\times\tilde{d})^{(2)}_{\mu} \quad (\mu=-2,-1,0,+1,+2) \tag{5}$$

is the s-d quadrupole operator. It is important to note that as the parameters ε_d, k, and χ change the Hamiltonian (3) describes spherical, deformed with axial symmetry, and, so called γ-unstable shapes, as extensively discussed in Chap. 3 of Ref. 7. The notation in Eqs. (4) and (5) is the standard notation for scalar products $(\cdot)$ and tensor products $(\times)$, i.e.,

$$(d^{\dagger}\times\tilde{d})^{(2)}_{\mu} = \sum_{\mu_1,\mu_2} (2,\mu_1,2,\mu_2|2,\mu) d^{\dagger}_{\mu_1}\tilde{d}_{\mu_2} . \tag{6}$$

Returning to Eq. (1), we take

$$\hat{H}_P = \sum_{i=1}^{2} \varepsilon_{p_i}\hat{n}_{p_i} , \tag{7}$$

where $\hat{n}_{p_i}$ is the number operator for p bosons of type i, and ε_{p_i} is the plasmon frequency of boson i, in the absence of coupling to the surface modes. The coupling Hamiltonian is

$$\hat{V}_{B,P} = \sum_{i=1}^{2} k_i'[\hat{\mathbf{Q}}\cdot(p_i^{\dagger}\times\tilde{p}_i)^{(2)}] , \tag{8}$$

i.e., a quadrupole-quadrupole interaction between the low-lying modes and the dipole modes. The coupling strength k_i' could, in principle, depend on i, but we take it, for simplicity, to be independent of dipole type. In order to compute photoabsorption cross sections, we also need to know the transition operator. This operator is an electric dipole operator, $E1$, and can be written as

$$\hat{T}_{\lambda} = \sum_{i=1}^{2} q_i(p_i^{\dagger}+\tilde{p}_i)_{\lambda} \quad (\lambda=-1,0,+1) . \tag{9}$$

Again, the constant, q_i, could depend on i, but we take it to be independent, q, and such that $\hat{T}$ satisfies an assigned fraction, α, of the energy-weighted sum rule,[13]

$$\sum_n E_n |\langle 1_n^- \| \hat{T} \| 0_1^+ \rangle|^2 = \frac{3\hbar^2}{2m_e} N e^2 \alpha . \tag{10}$$

Here, 1_n^- stands for the nth dipole state, at energy E_n, obtained from the diagonalization of Eq. (1), and the reduced matrix element of $\hat{T}$ is defined through the Wigner-Eckart theorem as in Ref. 7. On the right-hand side, N is the number of valence electrons and m_e the electron mass.

Absorption and coherent elastic scattering of unpolarized radiation by a cluster can be calculated from the polarizability:

$$P_0(\omega) = \tfrac{1}{3}\sum_n |\langle 1_n^- \| \hat{T} \| 0_1^+ \rangle|^2 \left[\frac{1}{E_n - i(\Gamma_n/2) - \hbar\omega} + \frac{1}{E_n + i(\Gamma_n/2) + \hbar\omega} \right] , \tag{11}$$

where ω is the incident photon frequency and Γ_n the width of the 1_n^- state. The absorption cross section is given by the optical theorem

$$\sigma_{\rm abs}(\omega) = 4\pi(\omega/c)\,{\rm Im}(P_0) \tag{12}$$

and the coherent elastic scattering is

$$\sigma_{\rm sc}(\omega) = (8\pi/3)(\omega/c)^4 |P_0|^2 . \tag{13}$$

III. RESULTS

By making use of the model of Sec. II one can compute the photoabsorption cross section for sodium clusters

TABLE I. Interacting-boson-model parameters for $N=8-20$ sodium clusters. EWSR is the energy weighted sum rule, see Eq. (10).

	Cluster						
	Na_8	Na_{10}	Na_{12}	Na_{14}	Na_{16}	Na_{18}	Na_{20}
N_B	2	4	9	9	10	4	2
ε_d (eV)	0.01	0.01	0.01	0.01	0.01	0.01	0.01
k (eV)	−0.05	−0.05	−0.05	−0.05	−0.05	−0.05	−0.05
χ	−1.000	−0.400	−0.400	−0.300	−0.300	+0.500	+1.000
ε_{p_1} (eV)	2.10	2.10	2.25	2.25	2.25	2.45	2.45
S_1 (% EWSR)	3	25	40	40	28	47	43
ε_{p_2} (eV)	2.52	2.70	2.85	2.85	2.58	2.90	2.90
S_2 (% EWSR)	67	50	30	28	30	30	25
k' (eV)	+0.05	+0.05	+0.05	+0.05	+0.05	+0.05	+0.05

with $N=8-20$. The fragmentation of dipole strength is determined by the following three quantities. (i) the cluster structure (ε_d, k, χ); in nuclei, this is obtained from a knowledge of the low-lying spectrum; in sodium clusters the low-lying spectrum has not been measured; we therefore assume the simplest possible structure for the clusters, namely that it is spherical at the "magic numbers" $N=8$ and 20, and deformed in between. We keep the parameters ε_d and k in $\hat{H}_B$, constant, and vary χ as in the analogous situation in nuclei. We note that negative values of χ correspond to prolate ellipsoids, while positive values of χ correspond to oblate ellipsoids. In addition to the structure parameters (ε_d, k, χ), we need to know also the total boson number, N_B. In nuclei this number is related to the number of nucleon pairs in the valence shell. Surprisingly, it appears that also here the number N_B as determined from a fit to experiment is related to the number of electron pairs in the valence shell. (ii) The next quantity that enters in the calculation of the photoabsorption spectrum is the plasmon energy, ε_{p_i}. Within small variations ($\pm 10\%$) these energies should be identical in all clusters in a shell ($N=8-20$). (iii) Finally, the last quantity is the strength of the coupling, k'.

In this first, empirical, study we have kept ε_d, k, and k' constant for all clusters, and allowed only χ and N_B to vary, and, within certain margins, the plasmon properties. Our results are shown in Table I. With the parameters of Table I, we have calculated the fragmentation of the dipole strength, as shown, for example, in Fig. 1. This fragmented spectrum, often called the "stick spectrum" is then spread over the underlying, more complex configurations by assigning to each fragment, 1_n^-, a width Γ_n. The width Γ_n is given by $\Gamma_n \equiv \Gamma(E_n)$, with

$$\Gamma(E)=0.11E \ , \tag{14}$$

where $\Gamma(E)$ and E are both measured in eV. The increase of the spreading width with energy, takes into account, both here and in the corresponding nuclear case, the increase of the underlying density of states with E, since, according to statistical theory,

$$\Gamma(E)=2\pi\rho(E)\langle v(E)\rangle^2 \ , \tag{15}$$

where $\rho(E)$ is the density of states at energy E and $\langle v(E)\rangle$ the average matrix element.

The energies of the fragments, E_n, and the dipole matrix elements, $\langle 1_n^- \| \hat{T} \| 0_1^+ \rangle$, have been obtained by numerical diagonalization of the IBM Hamiltonian (1), using the GR–GRT chain of codes.[14] The calculated photoabsorption cross sections per electron, $\sigma_{\rm abs}/N$, are compared with the experimental data in Figs. 2 and 3. In Fig. 4 we show the predicted scattering cross sections per electron, $\sigma_{\rm SC}/N$, versus the incident photon wavelength λ for some clusters. From Figs. 2 and 3, one can see that one can achieve an excellent description of all sodium clusters in the range $N=8-20$ within the framework of the present model. In other words, the splitting of the surface-plasma resonance due to the coupling with other electronic states (or to the underlying molecular structure), together with the splitting of these states due to the axial deformation of the cluster, is able to explain the available data. There does not seem to be any need to invoke triaxial deformations. [Note that triaxiality in nuclei seems to come from the fact that one has protons and

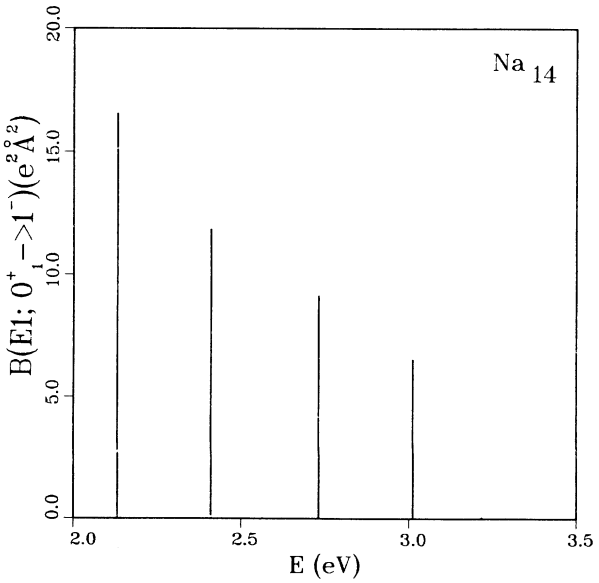

FIG. 1. Fragmentation of the dipole strength $B(E1, 0_1^+ \rightarrow 1^-)=|\langle 1_n^- \| \hat{T} \| 0_1^+ \rangle|^2$ in Na_{14}.

neutrons. The protons tend to produce an oblate deformation, while the neutrons tend to produce a prolate deformation (or vice versa). This is due to the neutron excess that puts protons and neutrons in *different* shells. The combination of these different deformations leads to triaxial shapes. In clusters we have only one type of particles. Hence, it is unlikely that we will obtain, from a microscopic calculation, triaxial shapes.]

We also comment briefly on the relation between the results obtained here and those reported in Ref. 2. Using the methods discussed in Chap. 3 of Ref. 7, it is possible to associate with each cluster a distortion parameter, δ. This is done by first evaluating the energy surface,

$$E(N_B;\beta,\gamma)=\langle N_B;\beta,\gamma|\hat{H}_B|N_B;\beta,\gamma\rangle \ , \tag{16}$$

where β,γ are the Bohr variables describing the ellipsoid (2), and then finding the equilibrium deformation, β_e, by minimizing $E(N_B;\beta,\gamma)$ with respect to β and γ. For axially symmetric ellipsoids, $\gamma=0°$ (prolate) or 60° (oblate). With the Hamiltonian (3), the equilibrium deformation β_e is approximately given by[15]

$$\beta_e \simeq \begin{cases} \frac{1}{2}[-(\frac{2}{7})^{1/2}+(\frac{2}{7}\chi^2+4)^{1/2}], & \chi\leq 0, \quad \text{prolate} \\ \frac{1}{2}[+(\frac{2}{7})^{1/2}\chi+(\frac{2}{7}\chi^2+4)^{1/2}], & \chi\geq 0, \quad \text{oblate} \ . \end{cases} \tag{17}$$

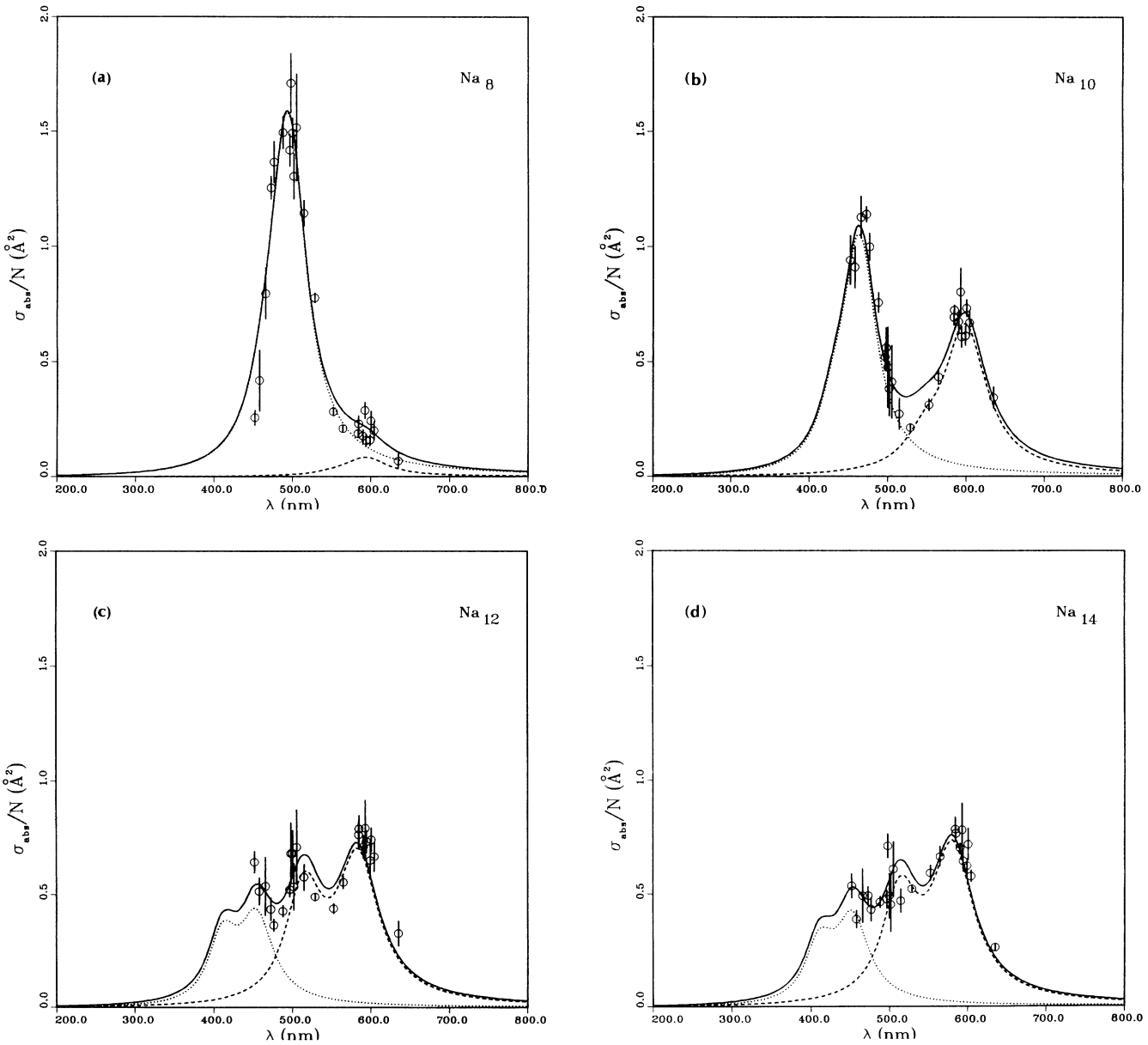

FIG. 2. Comparison between experimental (Ref. 1) and calculated total photoabsorption cross sections in sodium microclusters with a number of atoms ranging from $N=8$ to 14. The dashed curves represent the contributions of the two plasmon modes. The solid line represents the total contribution.

TABLE II. Equivalent distortion parameters of Na_8–Na_{20} clusters.

	N						
	8	10	12	14	16	18	20
δ^a	0.043	0.074	0.167	0.163	0.181	−0.076	−0.043
δ^b	0	0.44		−0.50		−0.24	0

[a]Present calculation.
[b]From Ref. 2.

The distortion parameter, δ, is related to N_B and β_e by

$$\delta = \begin{cases} cN_B\beta_e, & \text{prolate} \\ -cN_B\beta_e, & \text{oblate} \end{cases} \tag{18}$$

where the constant c is a scale factor. This scale factor can be determined by requiring that for a given value of N_B and β_e the IBM Hamiltonian produces the same splitting of a plasmon mode of unperturbed energy ω_M as a classical ellipsoid, i.e.,[3]

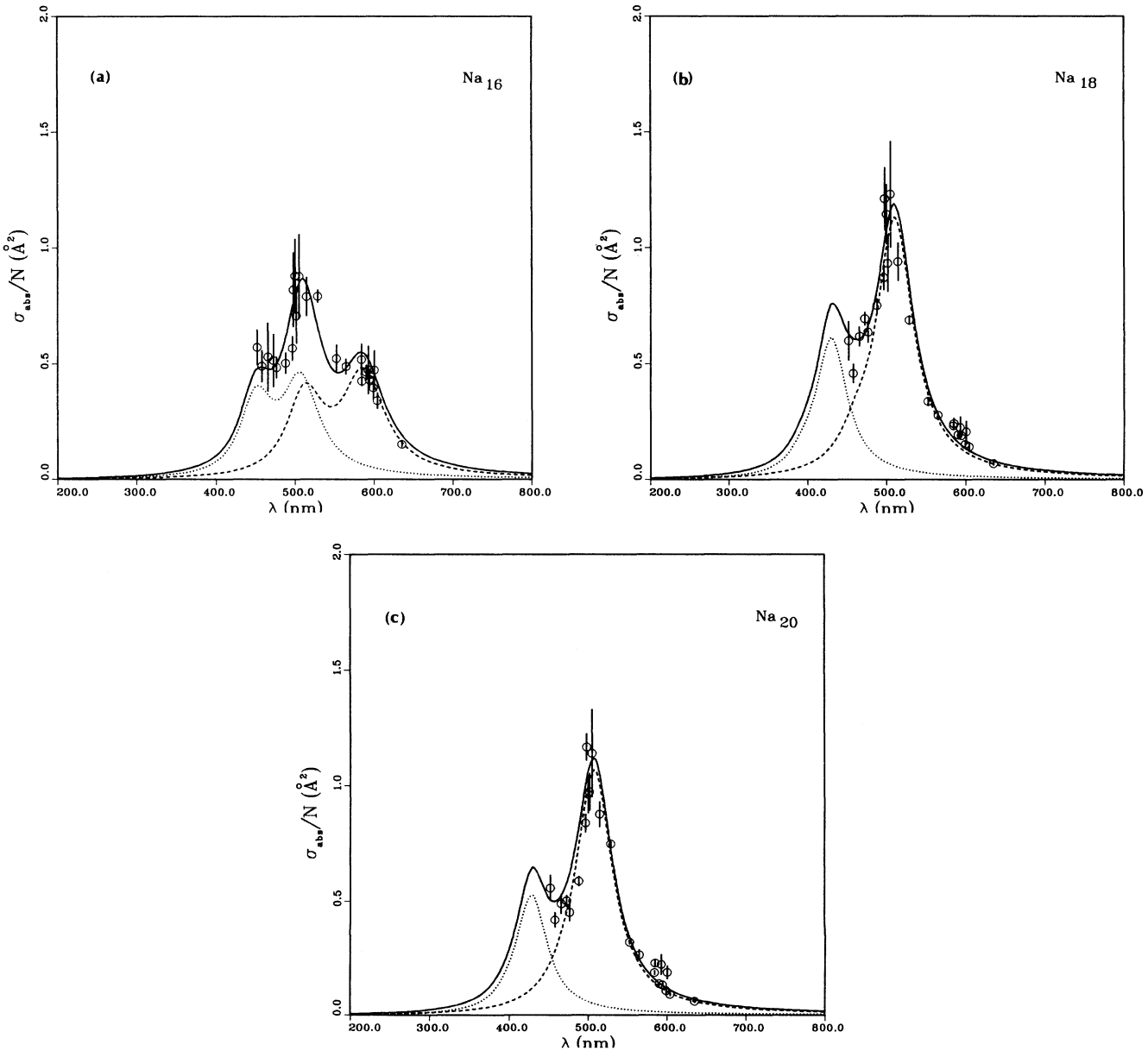

FIG. 3. Same as in Fig. 1, with $N = 16, 18, 20$.

$$\omega_z = \omega_M(1-\tfrac{2}{5}\delta) ,$$
$$\omega_x = \omega_y = \omega_M(1+\tfrac{1}{5}\delta) . \quad (19)$$

This gives $c=0.0167$. With this value, we can compute the distortion parameters given in the second row of Table II. These distortion parameters are typically smaller than those of Ref. 2 (see the third row of Table II), although they follow the same trend, i.e., prolate at the beginning of the shell and oblate at the end. They are also very similar to the values of the distortion parameters in atomic nuclei. It should be noted that, while for $N \geq 12$ we were unable to obtain a good fit of the data with only one plasmon mode, we were able to obtain a good fit for Na_{10} with only *one* plasmon mode. This fit required a distortion parameter of $\delta=0.33$ corresponding to $N_B=14$ and $\chi=-1.323$. We think that this unusually large distortion of a cluster with only two electrons in the valence shell is difficult to justify and not in line with the remaining clusters $N=8$ and 12–20. Thus, either Na_{10} has a peculiar structure that abruptly changes starting with $N=12$, or the interpretation in terms of two dipole modes applies to this cluster as well as to the others.

IV. CONCLUSIONS AND OUTLOOK

We have presented here a study of the splitting of plasma resonances in medium-size sodium clusters and related this to the structure of the cluster by making use of the interacting boson model. Independently from the particular choice of the parameters used in this paper, we

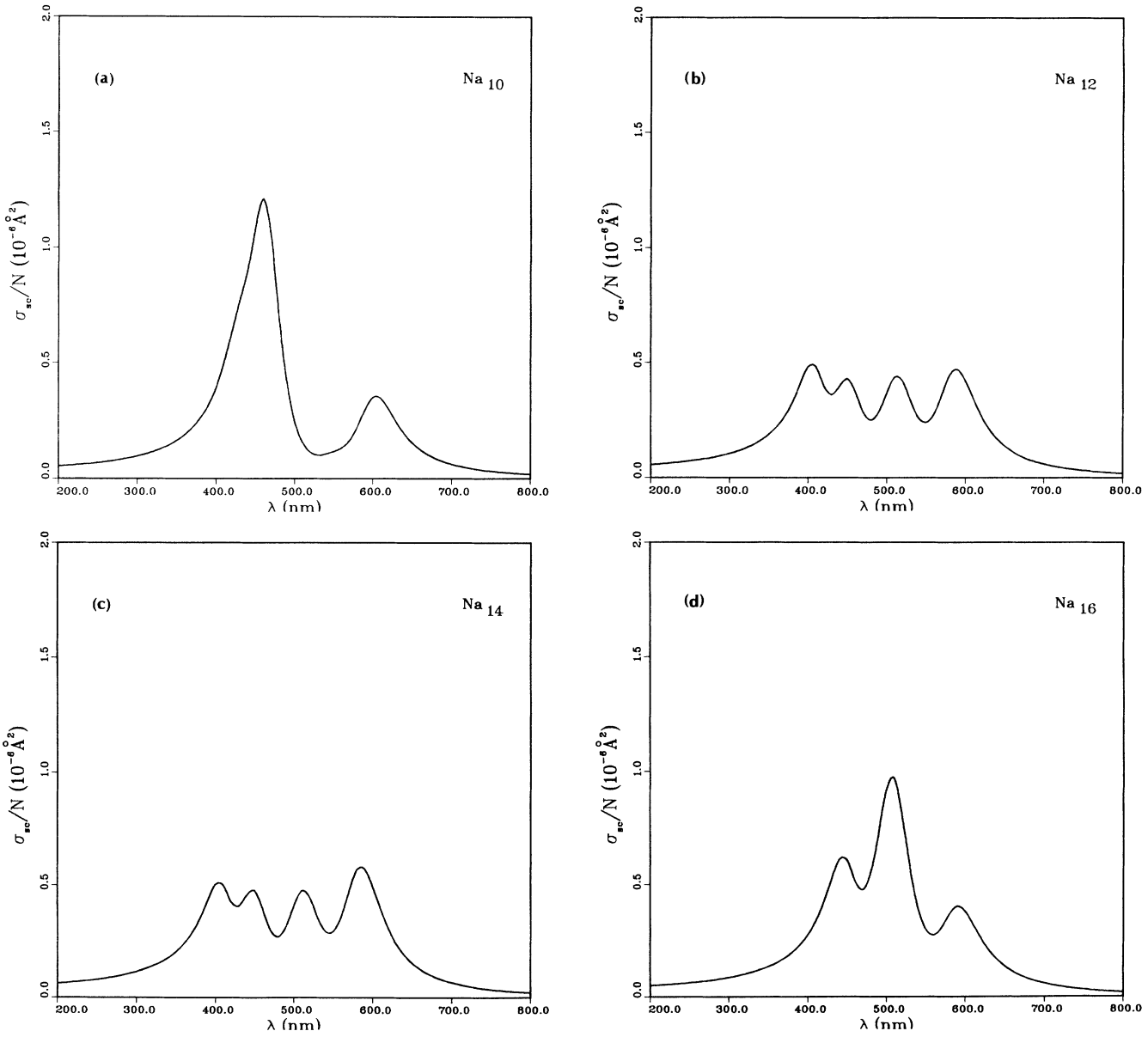

FIG. 4. Predicted elastic-scattering cross sections in $N=10$–20 sodium microclusters.

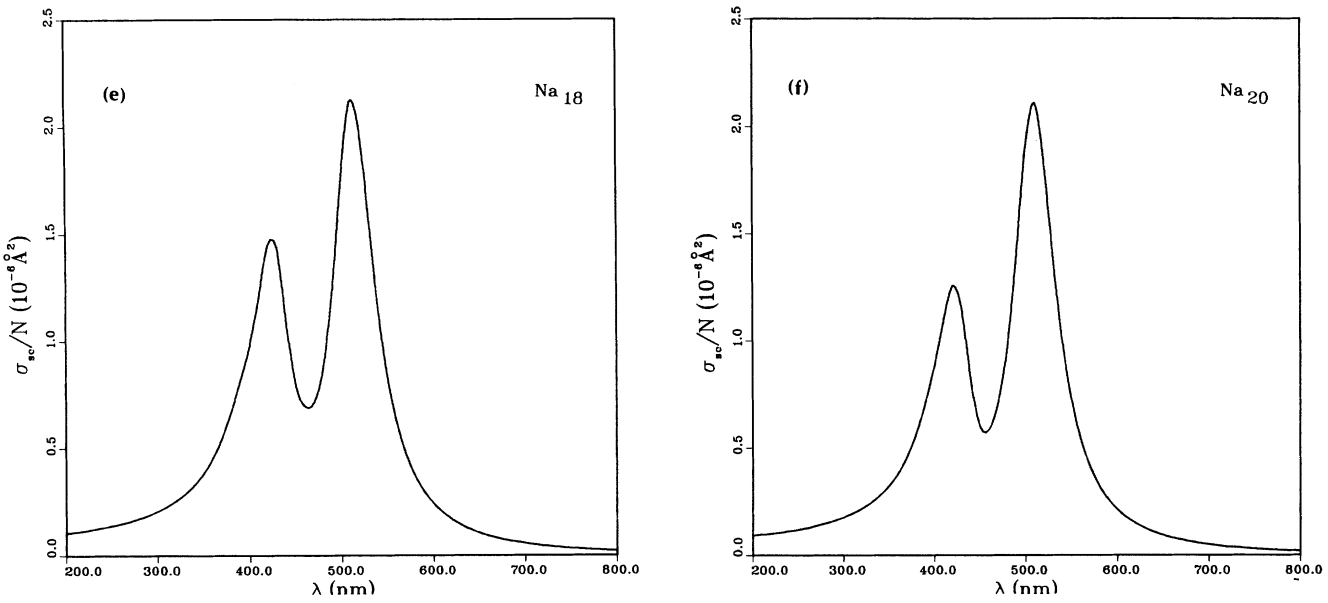

FIG. 4. (*Continued*).

think that, in general, algebraic models provide a natural framework for studying the complicated interplay between molecularlike, dropletlike, and crystal-like structure of metallic clusters. Here we have analyzed only the dropletlike aspect. A study of the molecularlike and crystal-like aspects is planned to be presented elsewhere. The molecularlike aspect is particularly relevant for small clusters, $N=2-8$. We believe that an understanding of how the molecularlike and dropletlike aspects merge into each other is of crucial importance for future studies of metallic clusters. *Ab initio* calculations of sodium clusters[6] produce cluster structures that are different from those of the droplet model. By studying the splitting of the plasmon mode for the two different structures and comparing with experiment, we may be able to tell the difference. In this respect, it would be important to perform a *high-resolution* study of an intermediate-size cluster, for example, $N=14$, covering a wavelength range as wide as possible (at least, from 430 to 830 nm), similar to that reported recently[16] for $N=4$ and 8. We have already computed, at least semiquantitatively, the splitting of the plasmon mode in presence of a variety of molecularlike structures, for example, tetrahedral and octahedral structures (T_d and O_h groups). It would be also of crucial importance to measure the low-lying electronic spectrum. The droplet model, as well as the molecular model, make definite predictions on how the low-lying electronic spectrum should look. We present in Fig. 5 a portion of the predicted droplet electronic spectrum of the $N=14$ cluster. The quantum numbers of the states are, in the droplet model, the electronic total orbital angular momentum and parity. To complete the description of the states, one should add the total spin quantum numbers. For $N=14$, with six electrons in the valence droplet shell, the spin values are $S=3,2,1,0$. The role of the electron spin the properties of the plasmon resonances has not yet been fully investigated. If the analogy between atomic nuclei and metal clusters persists at the spin level, the lowest states of a droplet with an even number of electrons have all $S=0$ (i.e., the electronic spins are paired). Further properties of the spin can be investigated in a relatively simple fashion within the framework of the interacting boson model by introducing s and d bosons with spin 0 and 1, as in the analogous nuclear case.[17] A detailed analysis of the situation is planned to be presented elsewhere. Here we only wish to contrast the droplet spectrum of Fig. 5 with molecularlike spectra, for example, with Fig. 1 of Ref. 6(b). One

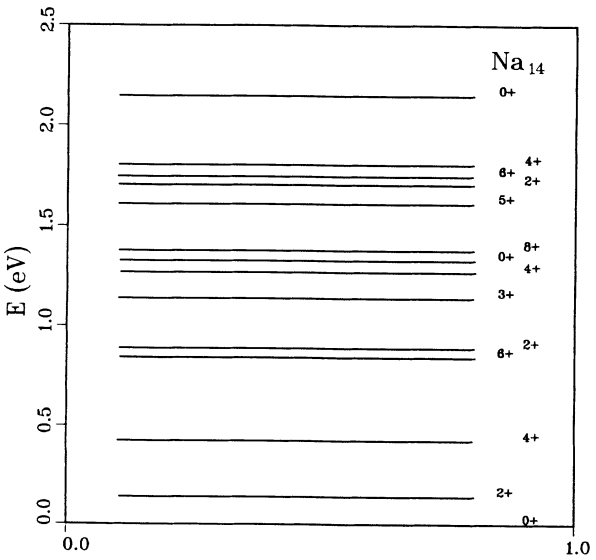

FIG. 5. IBM low-lying (positive-parity) electronic spectrum of Na_{14}. The orbital angular momentum and parity of the states is indicated to the right of each level.

can see that the two low-lying spectra are very different, despite the fact that one can make the absorption spectrum in the range 450–630 nm agree with data in both cases. A measurement of the low-lying electronic spectra is thus a key to a full understanding of metallic clusters.

Finally, we note that the fact we have obtained a good description of the available data in terms of a system of interacting bosons suggests an interpretation of the bosons as correlated electron pairs[18] (Cooper pairs). If this is the case, the adjustable parameters used here for reproducing the data can be derived from a fully microscopic calculation, similar to that performed for atomic nuclei. Also, in this case, the large-particle limit, $N \rightarrow \infty$, can be easily studied since it corresponds to the large-N limit of the interacting boson model.[7]

ACKNOWLEDGMENTS

This work was supported in part by the U.S. Department of Energy under Grant No. DE-FG02-91ER40608.

*Permanent address: Center for Theoretical Physics, Yale University, New Haven, CT 06511.

[1]K. Selby, V. Kresin, J. Masui, M. Vollmer, A. W. de Heer, A. Scheidemann, and W. D. Knight, Phys Rev. B **43**, 4565 (1991); K. Selby, V. Kresin, J. Masui, M. Vollmer, A. Scheidemann, and W. D. Knight, Z. Phys. D **19**, 43 (1991); K. Selby, Ph.D. thesis, University of California, Berkeley (1990).

[2]K. Selby, M. Vollmer, J Masui, V. Kresin, A. W. de Heer, and W. D. Knight, Phys. Rev. B **40**, 5417 (1989), and references therein.

[3]K. Clemenger, Phys. Rev. B **32**, 1359 (1985); E. Lipparini and S. Stringari, Z. Phys. D **18**, 193 (1991).

[4]C. Yannouleas, R. Broglia, M. Brack, and P. F. Bortignon, Phys. Rev. Lett. **63**, 255 (1989); C. Yannouleas, J. M. Pacheco, and R. A. Broglia, Phys. Rev. B **41**, 6088 (1990).

[5]V. Kresin, Z. Phys. D **19**, 105 (1991).

[6](a) V. Bonačić-Koutecký, P. Fantucci, and J. Koutecký, Phys. Rev. B **37**, 4369 (1988); (b) Chem. Phys. Lett **166**, 32 (1990).

[7]F. Iachello and A. Arima, *The Interacting Boson Model* (Cambridge University Press, Cambridge, 1987).

[8]F. Iachello, Chem. Phys. Lett. **78**, 581 (1981); F. Iachello and R. D. Levine, J. Chem. Phys. **77**, 3046 (1982).

[9]J. M. Pacheco, R. A. Broglia, and B. R. Mottelson (unpublished).

[10]G. Maino, A. Ventura, L. Zuffi, and F. Iachello, Phys. Rev. C **30**, 2191 (1984); Phys. Lett. B **152**, 17 (1985).

[11]F. Iachello and P. Van Isacker, *The Interacting Boson-Fermion Model* (Cambridge University Press, Cambridge, 1991), Chap. 12.

[12]G. Maino, A. Ventura, and L. Zuffi, Phys. Rev. C **37**, 1379 (1988).

[13]E. Lipparini and S. Stringari, Phys. Rep. **175**, 103 (1989), and references therein.

[14]P. Van Isacker, computer codes GR and GRT (unpublished).

[15]J. N. Ginocchio and M. W. Kirson, Nucl. Phys. A **350**, 31 (1980).

[16]C. R. C. Wang, S. Pollack, and M. M. Kappes, Chem. Phys. Lett. **166**, 26 (1990).

[17]J. P. Elliott and J. A. Evans, Phys. Lett. **101B**, 216 (1981).

[18]F. Iachello, E. Lipparini, and A. Ventura (unpublished).